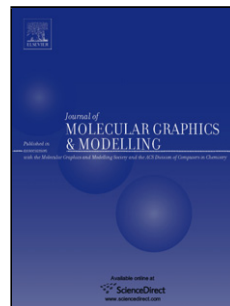


Accepted Manuscript

Title: Theoretical study on the *N*-demethylation mechanism of theobromine catalyzed by P450 isoenzyme 1A2

Author: Jing Tao Yuan Kang Zhiyu Xue Yongting Wang Yan
Zhang Qiu Chen Zequin Chen Ying Xue



PII: S1093-3263(15)30020-6

DOI: <http://dx.doi.org/doi:10.1016/j.jmgm.2015.06.017>

Reference: JMG 6572

To appear in: *Journal of Molecular Graphics and Modelling*

Received date: 12-3-2015

Revised date: 24-6-2015

Accepted date: 25-6-2015

Please cite this article as: Jing Tao, Yuan Kang, Zhiyu Xue, Yongting Wang, Yan Zhang, Qiu Chen, Zequin Chen, Ying Xue, Theoretical study on the *N*-demethylation mechanism of theobromine catalyzed by P450 isoenzyme 1A2, *Journal of Molecular Graphics and Modelling* <http://dx.doi.org/10.1016/j.jmgm.2015.06.017>

This is a PDF file of an unedited manuscript that has been accepted for publication. As a service to our customers we are providing this early version of the manuscript. The manuscript will undergo copyediting, typesetting, and review of the resulting proof before it is published in its final form. Please note that during the production process errors may be discovered which could affect the content, and all legal disclaimers that apply to the journal pertain.

Theoretical Study on the N-Demethylation Mechanism of Theobromine Catalyzed by P450 Isoenzyme 1A2

Jing Tao^{a,†} Yuan Kang^{a,†} Zhiyu Xue^a Yongting Wang^a Yan Zhang^a
Qiu Chen^a Zequin Chen^{a,*} Ying Xue^b

^aCollege of Chemistry and Chemical Engineering,
Chemical Synthesis and Pollution Control Key Laboratory of Sichuan Province,
China West Normal University, Nanchong 637002,
People's Republic of China
^bCollege of Chemistry,
Key Laboratory of Green Chemistry and Technology in Ministry of Education,
Sichuan University, Chengdu 610064,
People's Republic of China

Highlights

- The N-demethylation mechanisms of theobromine catalyzed by CYP1A2 were explored using the unrestricted B3LYP theory;
- The rate-limiting N-methyl hydroxylation occurs in a HAT mechanism;
- The carbinolamines generated are prone to decomposition through the contiguous heteroatom-assisted proton transfer;
- The N-demethylation reaction proceeds through a SSM mechanism and HS is more favorable than LS;
- 3-N demethylation is kinetically more feasible than 7-N demethylation and 7-methylxanthine is the optimum metabolite of theobromine.

Graphical abstract

Abstract

Theobromine, a widely consumed pharmacological active substance, can cause undesirable muscle stiffness, nausea and anorexia in high doses ingestion. The main N-demethylation metabolic mechanism of theobromine catalyzed by P450 isoenzyme 1A2 (CYP1A2) has been explored in this work using the unrestricted hybrid density functional

* Corresponding author. E-mail address: chenzeqin@cwnu.edu.cn
Phone: +86-817-2568081

†These authors contributed equally to this work.

method UB3LYP in conjunction with the LACVP(Fe)/6-31G (H, C, N, O, S, Cl) basis set. Single-point calculations including empirical dispersion corrections were carried out at the higher 6-311++G** basis set. Two N-demethylation pathways were characterized, i.e., 3-N and 7-N demethylations, which involve the initial N-methyl hydroxylation to form carbinolamine complexes and the subsequent carbinolamines decomposition to yield monomethylxanthines and formaldehydes. Our results have shown that the rate-limiting N-methyl hydroxylation occurs via a hydrogen atom transfer (HAT) mechanism, which proceeds in a spin-selective mechanism (SSM) in the gas phase. The carbinolamines generated are prone to decomposition via the contiguous heteroatom-assisted proton-transfer. Strikingly, 3-N demethylation is more favorable than 7-N demethylation due to its lower free energy barrier and 7-methylxanthine therefore is the optimum product reported for the demethylation of theobromine catalyzed by CYP1A2, which are in good agreement with the experimental observation. This work has first revealed the detail N-demethylation mechanisms of theobromine at the theoretical level. It can offer more significant information for the metabolism of purine alkaloid.

Keywords: Theobromine; N-demethylation mechanism; CYP1A2; Metabolism; Density function theory; dispersion correction

1. Introduction

Theobromine, known as 3,7-dimethylxanthine, naturally exists in tea leaves, coffee beans, theobroma cacao plant and cola nuts, etc [1-3]. It also exists as one of the important metabolite of caffeine [4]. Theobromine has attracted considerable attention all the time since it can cause various physiological effects. It shares in common with caffeine and theophylline in pharmacological actions, such as attention, mood and vigilance [5, 6]. Its function on the central nervous system, to some extent, is weaker than caffeine and theophylline [7, 8]. Theobromine also displays application as a diuretic and smooth muscle relaxant and has the functions of vasodilatation and myocardial stimulation [9, 10]. These make it widely be applied to food and drug products, e.g., coffee, chocolate, non-alcoholic beverage as well as antitussive and bronchodilator [11-13]. Nevertheless, the ingestion of high doses of theobromine can cause undesirable symptoms, such as, muscle stiffness, nausea and anorexia [9]. As people intake theobromine from foods or drugs easily everyday, it is essential to investigate the metabolic property of theobromine in human.

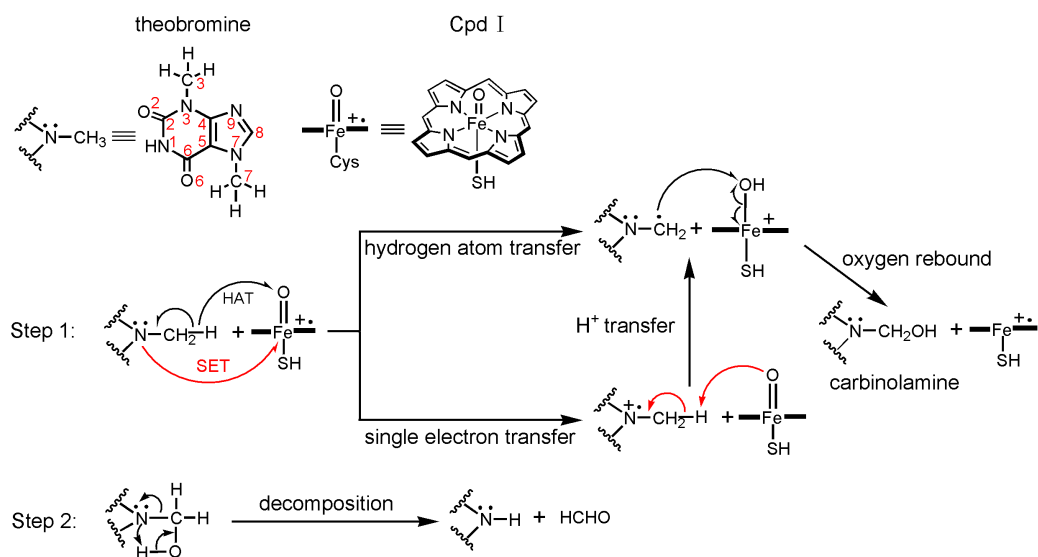
Several biological enzymes, such as cytochrome P450 proteins (CYPs) and xanthine oxidase (XOD), play an important role in the metabolism of theobromine. CYPs are well known as all-purpose biocatalysts, because they are involved in many reactions, such as, N-, O-, and S-dealkylation and oxidation, C–H hydroxylation in saturated hydrocarbons and N-hydroxylation [14]. P450 isoenzyme 1A2 (CYP1A2) enzyme belongs to the CYP1A subfamily which constitutes about 15% of the entire liver cytochrome P450 content in human [15]. Its activity is significant for the metabolism of various drugs and for the biotransformation of physiologically important endogenous compounds, e.g., caffeine, theophylline, theobromine phenacetin, imipramine, phenothiazine neuroleptics, propranolol, clozapine, melatonin and steroids [16-18]. Additionally, It plays an important role in the activation of procarcinogens, such as, mycotoxin aflatoxin B1 (AFB1) [19, 20].

Catalyzed by CYP1A2, the main metabolism of theobromine commences via N-demethylation [21]. By the 3-N and 7-N demethylations, 7-methylxanthine and 3-methylxanthine are generated, respectively [22]. When a dose of theobromine is ingested, approximately 10% theobromine is excreted in the urine unchanged, whereas approximately 60% and 20% theobromine are excreted in the forms of 7-methylxanthine and 3-methylxanthine, respectively [23]. The study of Rodopoulos and his co-workers have also shown that 7-methylxanthine formation represented about 34–48% of total biotransformation via CYP1A2, whereas 3-methylxanthine constituted 20% [24]. As can be readily seen, N-demethylation metabolism of theobromine catalyzed by CYP1A2 is significantly important.

The overall reaction of P450-catalyzed *N*-demethylation proceeds via two steps (Scheme

1), the methyl hydroxylation (step 1) followed by the fission of the C-N bond to release formaldehyde (step 2). Two putative mechanistic options have been adopted for the N-methyl hydroxylation, i.e., hydrogen atom transfer (HAT) [25, 26] and single-electron transfer (SET) [27]. Originating from the high-spin (HS) quartet and low-spin (LS) doublet states of the active species of CYP1A2 (Compound I, Cpd I in brief), theoretical studies on the initial N-methyl hydroxylation of alkane have explored two possible mechanisms: the two-state reactivity (TSR) scenario [28-30] and the spin-selective manner (SSM) [31, 32].

Scheme 1. Proposed N-demethylation mechanism of theobromine catalyzed by CYP1A2.



As the principal metabolism pathway of theobromine, N-demethylation mechanism, to the best of our knowledge, remain many intriguing questions. Such as, which mechanism does theobromine *N*-demethylation favor, HAT or SET? Does the multiplicity of Cpd I have decisive effect on the mechanism? And then, which pathway is the most favorable for the C-N bond fission? Quantum chemistry has been widely adopted at present to provide more useful information about short-lived transition states that is difficult to obtain from experiments. The present work is aimed at clarifying the above questions to offer the missing insight and reveal mechanistic details at the theoretical level. The results obtained can provide more useful information about the metabolism of purine alkaloid and lay the foundation for theoretical research of N-dealkylation reactions catalyzed by CYP1A2.

2. Computational details

The computational reaction model employed comprises 61 atoms and consists of the two parts: (a) theobromine and (b) Cpd I of CYP1A2, a six-coordinate oxo-ferryl species including a truncated heme and a thiolate axial ligand (SH-) built from the crystal structure of CYP1A2 (PDB: 2HI4) [33]. Standard procedures within the Gauss View program were used

to build an input file via incorporating these coordinates [34].

All DFT calculations presented here were carried out with the Gaussian 09 suite of programs [35]. Geometries for all the stationary points, including the reactant complex (RC), product complex (PC), intermediate (IM), and transition state (TS), were fully optimized in the gas phase using the unrestricted hybrid density functional method UB3LYP in conjunction with the LACVP(Fe)/6-31G(H, C, N, O, S, Cl) basis set (B1 in brief). Transition states were affirmed by harmonic frequency analysis to possess only one imaginary frequency and the stationary points were confirmed as minima with all positive frequencies. The connectivity between the stationary points was established by intrinsic reaction coordinate (IRC) calculations [36, 37]. Natural Population Atomic (NPA) charges were determined with the Natural Bond Order (NBO) analysis of Reed and Weinhold. To gain more reliable energies, single-point calculations were performed using UB3LYP and dispersion corrected UB3LYP-D3 at two higher basis sets, 6-311+G* and 6-311++G** (B2 and B3 in brief). In order to further examine the computational results, a series of single-point calculations were carried out using two other dispersion corrected functionals including B3PW91-D3 and PBE1PBE-D3 with B3 basis set to evaluate the free energy barriers for the rate-determining steps.

3. Results and discussion

For theobromine, two possible demethylation pathways were identified, i.e., 3-N and 7-N demethylations, denoted as paths A and B, respectively. Both of them commence via the N-methyl hydroxylation. The general model of N-methyl hydroxylation involves the proton transfer from methyl group to the oxygen atom of Cpd I to generate a N-methylene intermediate, which acts as receptor of a hydroxyl from the active iron species via oxygen-rebound process.

3.1 N-Methyl hydroxylation of theobromine

3.1.1 Geometric features

N₃-Methyl hydroxylation The optimized geometries of all the stationary points for N₃-methyl hydroxylation of theobromine are shown in Fig. 1. On the LS doublet state, the N₃-methyl hydroxylation is concerted in the gas phase, directly leading to the formation of carbinolamine (3-methylol-7-methylxanthine)-heme complex, A⁻²IM_H, without a distinct oxygen-rebound step. The located transition state A⁻²TS_H is characterized by its single imaginary frequency of 400.6i cm⁻¹, which mainly corresponds to the proton (H) transfer from N₃-methyl carbon atom to the oxygen atom of Cpd I. Compared with the reactant complex, A⁻²RC, it can be seen that in A⁻²TS_H, the Fe–O bond is lengthened by 0.136 Å, while the O–H distance is reasonably reduced by 1.576 Å. These are concurrent with the elongation of the C₃–H bond by 0.369 Å and the curtailment of the C₃–N₃ bond by 0.089 Å. In A⁻²TS_H, the

arrangement of the C₃-H-O atoms is almost collinear with the bond angle of 163.71°. The hydrogen atom is closer to the oxygen atom ($r_{O-H}=1.081 \text{ \AA}$) than to the carbon atom ($r_{C3-H}=1.463 \text{ \AA}$), therefore, more product-like in character.

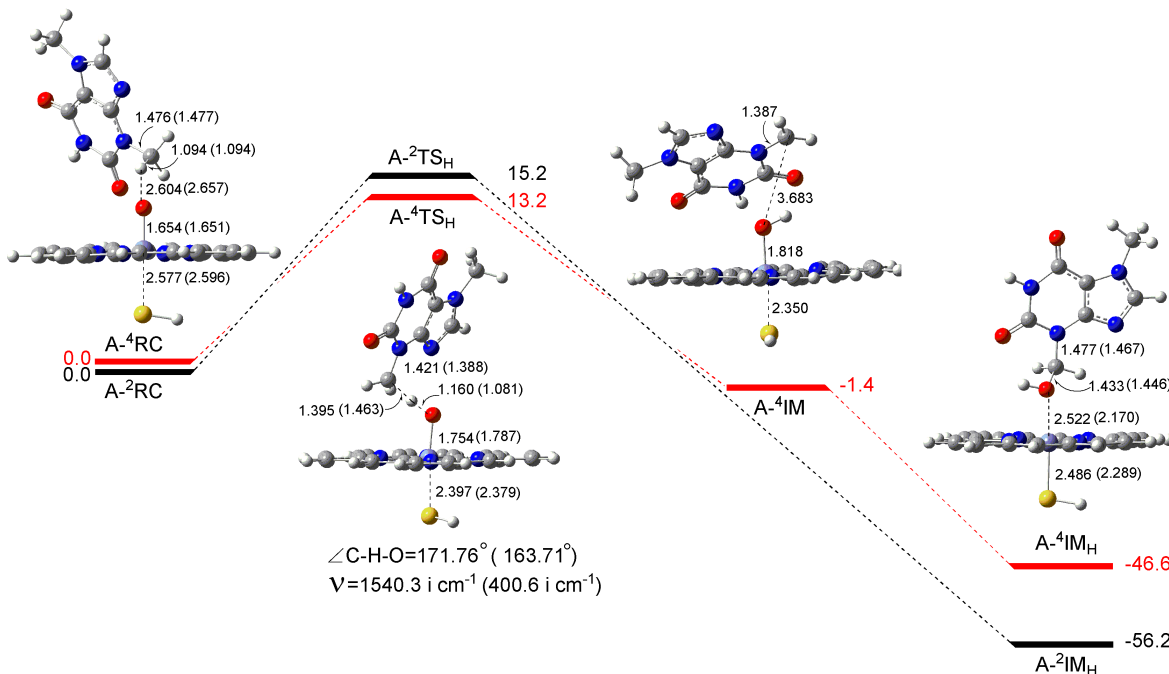


Fig. 1. Potential energy surfaces (in kcal mol^{-1}) and optimized structures (in \AA) for the N₃-methyl hydroxylation of theobromine (values in parentheses, geometrical parameters on the LS state; values out of parentheses, geometrical parameters on the HS state). Relative free energies are calculated at UB3LYP-D3 functional with B3 basis set. Definitions are the same in the figure 2.

Nevertheless, N₃-methyl hydroxylation on the HS quartet state has a distinct but barrier-free oxygen-rebound process. The single imaginary frequency (1540.3i cm^{-1}) of transition state A-⁴TS_H involved in the transfer of proton (H) from N₃-methyl carbon atom to the oxygen atom of Cpd I, leading to the formation of N-methylene intermediate, A-⁴IM. As can be seen from Figure 1, the geometrical feature tendencies from A-⁴RC to A-⁴TS_H are similar to those on the LS doublet state: the Fe–O bond is gradually lengthened by 0.100 \AA and the O–H distance is shortened by 1.444 \AA ; correspondingly, the C₃–H bond is elongated by 0.301 \AA and the C₃–N₃ bond is reduced by 0.055 \AA . In A-⁴TS_H, C₃-H-O atoms also exhibit collinear arrangement with the bond angle of 171.76°. The hydrogen atom is still nearer to the oxygen atom ($r_{O-H}=1.160 \text{ \AA}$) than to the carbon atom ($r_{C3-H}=1.395 \text{ \AA}$), thus, more product-like in character. And then, the N-methylene intermediate A-⁴IM formed acts as a shoulder but not a real minimum and falls to the carbinolamine-heme complex, A-⁴IM_H, with a barrier-free

oxygen rebound process. Compared with A-⁴IM, the Fe–O, Fe–S and C₃–N₃ distances in A-⁴IM_H have been elongated by 0.704, 0.136 and 0.090 Å, respectively, while the C₃–O distance has been reasonably reduced to be 1.433 Å. Consequently, the N₃–methyl hydroxylation of theobromine is concerted on both the LS doublet and HS quartet states, which keeps accordance with the previous observation on P450 reactions [32].

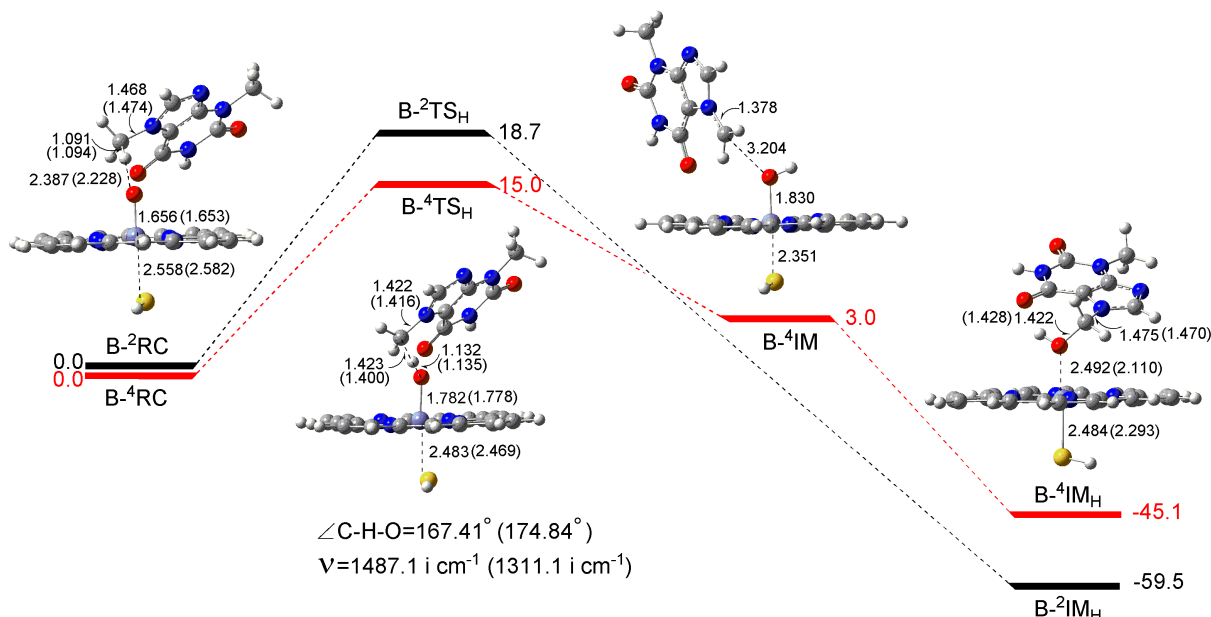


Fig. 2. Potential energy surfaces (in kcal mol⁻¹) and optimized structures (in Å) for the N₇–methyl hydroxylation of theobromine at UB3LYP-D3 functional with B3 basis set.

N₇-Methyl hydroxylation The optimized geometries of all the stationary points for N₇–methyl hydroxylation of theobromine are shown in Fig. 2. Analogous to N₃–methyl hydroxylation, N₇-methyl hydroxylation is still concerted on the LS doublet state, generating carbinolamine (7-methylol-3-methylxanthine)-heme complex, B-²IM_H. On the HS quartet state, the N₇-methyl hydroxylation still has a distinct but barrier-free oxygen-rebound process. Transition states involved are characterized by their single imaginary frequencies: 1311.1i cm⁻¹ for B-²TS_H on the LS doublet state and 1487.1i cm⁻¹ for B-⁴TS_H on the HS state, whose imaginary frequencies both correspond to the proton (H) transfer from the N₇-methyl carbon atom to the oxygen atom of Cpd I. Compared with the reactant complexes, B-^{2,4}RC_H species, the Fe–O bond in transition states, B-^{2,4}TS_H species, is gradually lengthened by 0.125 Å LS doublet state and 0.126 Å HS quartet state, while the O–H distance is reasonably reduced by 1.093 Å LS doublet state and 1.255 Å HS quartet state. Meanwhile, the C₇–H distance is elongated by 0.306 Å LS doublet state and 0.332 Å HS quartet state, followed by the curtailment of the C₇–N₇ bond by 0.058 Å LS doublet state and 0.046 Å HS quartet state. Both transition states B-²TS_H and B-⁴TS_H are distinguished by an almost collinear positioning

of the C₇-H-O atoms, with the bond angle of 174.84° and 167.41°, respectively. In B-²TS_H and B-⁴TS_H, the hydrogen atoms are also closer to the oxygen atoms ($r_{O-H, LS}=1.135 \text{ \AA}$, $r_{O-H, HS}=1.132 \text{ \AA}$) than to the carbon atoms ($r_{C7-H, LS}=1.400 \text{ \AA}$, $r_{C7-H, HS}=1.423 \text{ \AA}$), therefore, more product-like in character. On the HS quartet state, the next barrier-free oxygen rebound process is favorable to stabilize the N-methylene intermediate B-⁴IM, yielding carbinolamine-heme complex, B-⁴IM_H. As the reaction progresses from B-⁴IM to B-⁴IM_H, the bond lengths of Fe–O, Fe–S and C₇–N₇ have been elongated by 0.662 Å, 0.133 Å and 0.097 Å, respectively; concomitantly, the C₇–O distance has been reasonably reduced by 1.782 Å. As can be readily seen, the N₇–methyl hydroxylation is also concerted on both the LS doublet and HS quartet states.

3.1.2 Energetics

In order to theoretically examine the calculated free energy barriers, dispersion correction, basis set and functional tests were performed for the N-methyl hydroxylation step of theobromine. The calculated free energy barriers are collected in Table 1 for comparison. It is seen from Table 1 that the free energy barriers calculated at B3 basis set are systematically ca. 3 kcal mol⁻¹ lower than those at B2 basis set, indicating that the B2 basis set overestimated the free energy barriers. The dispersion corrected free energy barriers are uniformly lower than those without dispersion correction by 1.4~4.2 kcal mol⁻¹. So dispersion correction should be included in the calculation. Based on B3 level, the free energy barriers obtained using the B3PW91-D3 and PBE1PBE-D3 functionals are slightly lower compared with the UB3LYP-D3 functional. By using different dispersion corrected density functionals, the calculated energy barrier differences between N₃– and N₇–methyl hydroxylations range from 1.8 to 4.0 kcal mol⁻¹, as one can see in Table 1. Thus, no matter what functional is used, the DFT calculations can consistently predict the reactivity patterns and the conclusions drawn here. And therefore our following energetics discussions focus on the results obtained using UB3LYP-D3 functional with the B3 basis set.

As depicted in Table 1, the free energy barriers of A-²TS_H and A-⁴TS_H are predicted to be 15.2 and 13.2 kcal mol⁻¹, respectively. The energy gap between A-²TS_H and A-⁴TS_H is 2.0 kcal mol⁻¹. The ratio of the reaction rates on the LS:HS route is 1:28.6. It indicates that the N₃–methyl hydroxylation occurs via the SSM mechanism in the gas phase and kinetically proceeds mainly through the HS state. For N₇-methyl hydroxylation, the LS and HS free energy barriers are 18.7 and 15.0 kcal mol⁻¹, respectively. The energy gap between B-²TS_H and B-⁴TS_H is as large as 3.7 kcal mol⁻¹. The ratio of the reaction rates on the LS:HS route is 1:496.1. It indicates that the N₇–methyl hydroxylation occurs also via the SSM mechanism in

the gas and the HS is more favorable than LS from the kinetic point of view. Consequently, N₃-methyl hydroxylation is kinetically more favored than N₇-methyl hydroxylation in the N-demethylation of theobromine due to its lower free energy barrier.

The changes in free energy for the N-methyl hydroxylation of theobromine are depicted in Figs. 1 and 2. It shows that the N-methyl hydroxylation is greatly exothermic with reaction energies of more than 45 kcal mol⁻¹, suggesting that the N-methyl hydroxylation is thermodynamically favorable either on LS and HS. Considering the great higher stability of the intermediates formed by N-methyl hydroxylation compared with the reactant complexes, the energy barrier will determine the optimum reaction pathway. Thus N-methyl hydroxylation is predicted to be under kinetic control.

3.1.3 Electronic structural features for N–methyl hydroxylation

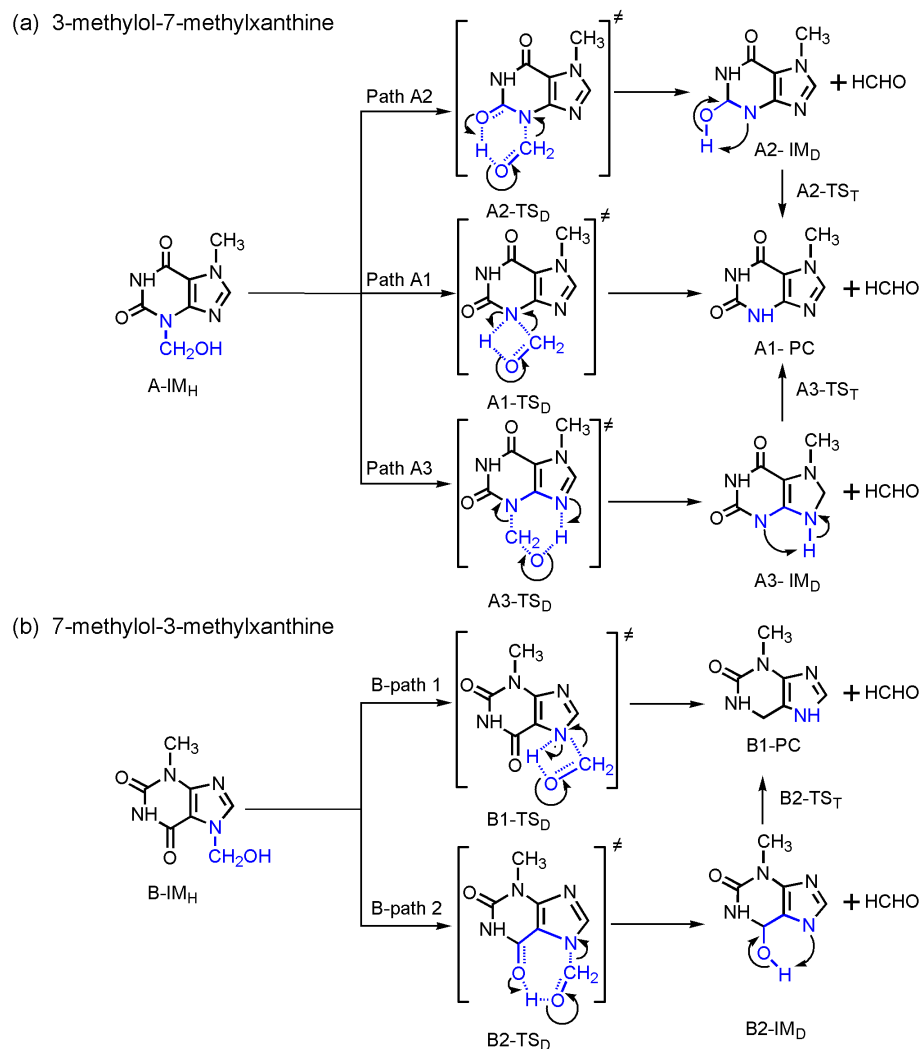
The calculated spin density distribution for the species in the N–methyl hydroxylation of theobromine is reported in Table 2. In the reactant complexes, ^{2,4}RC species, spin density mainly resides on the catalytic active center of Cpd I. At the C–H bond activation step, it partly shifts to theobromine. In the transition states, ^{2,4}TS_H species, high spin density resides on the alpha carbon and Fe-oxo species. The accumulation of spin density on carbon atom contributes to the stabilization of carbon atom during the proton transfer. In the N-methylene intermediates, ⁴IM species, with a significant amount of the spin density on theobromine delocalized in the direction of carbon, is in turn conjugated with the π orbital on the porphyrine group and forms a conjugated $\pi_{\text{pur}}-\pi_{\text{C-N}}$ orbital. There is also accumulation of the spin density on iron by a shift from –SH and oxygen. After the hydroxyl rebound step, spin density is primarily localized on iron. Consequently, the N–methyl hydroxylation of theobromine is initiated by a hydrogen atom transfer (HAT) step.

3.2 Fission of C–N bond

A carbinolamine-heme complex is formed at the end of the N–methyl hydroxylation. The next step along the N-demethylation of theobromine is the carbinolamine decomposition to yield methylxanthine and formaldehyde via the fission of C–N bond. With the low binding energy of carbinolamine to the heme (LS: 3.56 kcal mol⁻¹, HS: 0.12 kcal mol⁻¹ in path A; LS: 4.61 kcal mol⁻¹, HS: 1.46 kcal mol⁻¹ in path B) indicates that the generated carbinolamine then can rapidly dissociate from the active site of CYP1A2 and decomposes in a nonenzymatic environment [31]. So, nonenzymatic decomposition of the carbinolamine species is investigated in this section. Considering the presence of one auxiliary water molecule in the active active site of the human P450 1A2 [33], one-water-assisted reaction mechanism were taken into account for comparison when the direct reaction mechanism involves a

four-membered transition state with large ring strain.

Scheme 2. Proposed reaction pathways for the C-N fissions of 3-methylol-7-methylxanthine (a) and 7-methylol-3-methylxanthine (b).



3.2.1 Fission of C-N bond in 3-methylol-7-methylxanthine

In this step, 3-methylol-7-methylxanthine, A-IM_H, formed by N₃-methyl hydroxylation undergoes C-N bond fission to release 7-methylxanthine and formaldehyde. This process is actually a proton transfer process. According to the structure feature of A-IM_H, there are three possible pathways for the proton transfer denoted as paths A1, A2 and A3, respectively (Scheme 2a). The optimized geometries of all the stationary points for paths A1, A2 and A3 are shown in Fig. 3. The calculated energy profiles are depicted in Figs. 4 and 5.

Path A1

In path A1, the proton on the hydroxyl oxygen is directly transferred to N₃ atom, yielding the keto form structure of 7-methylxanthine and formaldehyde (A1-PC). The transition state A1-TS_D has a four-membered ring structure formed by N₃, C₃, O and H atoms (Fig. 3a). The distances of N₃-C₃, C₃-O, O-H and H-N₃ are 2.397, 1.306, 1.013 and 1.964 Å, respectively.

The free energy barrier of A1-TS_D is 53.3 kcal mol⁻¹ (Fig. 4a), which is so high that it is rather difficult for path A1 to occur directly. The large energy barrier mainly arises from the four-centered transition state, where the orbitals required for the bond dissociation and formation are deformed so much that a large amount of deformation energy is needed.

To relax the transition state and reduce the angle strain, the water-mediated proton transfer mechanism of path A1 is clarified with one auxiliary water molecule. With the assistance of the auxiliary water molecule, the located transition state A1-TS_{DW} is expanded to be a six-membered ring structure formed by N₃, C₃, O, H, O_w and H_{w1} atoms (Fig. 3a). The vector of the imaginary vibrational frequency of A1-TS_{DW} is mainly associated with the coupling of the transfer of H atom from O to O_w atoms and the transfer of H_{w1} atom from O_w to N₃ atoms, leading to the cleavage of the C₃-N₃ bond. The distances of N₃-C₃, C₃-O, O-H, H-O_w, O_w-H_{w1} and H_{w1}-N₃ are 2.097, 1.293, 1.229, 1.202, 1.101 and 1.448 Å, respectively. The free energy barrier of A1-TS_{DW} is 37.2 kcal mol⁻¹ (Fig. 4a), which, as expected, is decreased drastically by ca. 16.1 kcal mol⁻¹ in comparison with the direct reaction process. Even so, large energy barrier is still involved in the water-mediated path A1. Clearly, this proton transfer process is not feasible in the kinetic point.

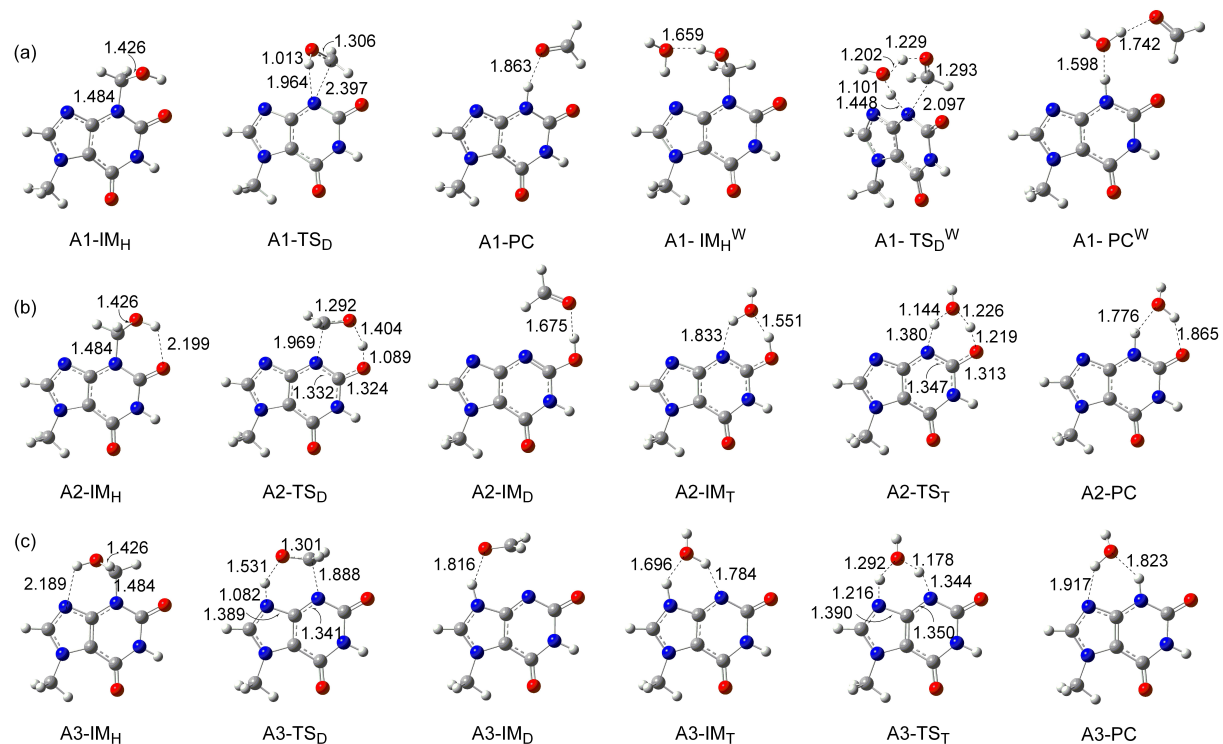


Fig. 3. Optimized structures of the stationary points for the nonenzymatic fission of C-N bond in 3-methylol-7-methylxanthine (bond length in Å).

Path A2

As depicted in Scheme 2a, path A2 is a two-step pathway. It initially involves the proton transfer from the hydroxyl oxygen to the contiguous heteroatom O₂ atom, forming the O₂-enol form structure of 7-methylxanthine and formaldehyde (A2-IM_D), which undergoes subsequent enol-to-keto tautomerism to yield the stable keto form structure of 7-methylxanthine (A2-PC). For the first proton transfer step, the located transition state A2-TS_D is a six-membered ring structure formed by N₃, C₃, O, H, O₂ and C₂ atoms (Fig. 3b). The vector of the imaginary vibrational frequency for the transition state A2-TS_D is mainly associated with the transfer of the proton (H) from O to O₂ atom with the simultaneous breakage of N₃-C₃ bond. The distances of N₃-C₃, C₃-O, O-H, H-O₂, O₂-C₂, and C₂-N₃ are 1.969, 1.292, 1.404, 1.089, 1.324 and 1.332 Å, respectively. The free energy barrier of A2-TS_D is predicted to be 23.9 kcal mol⁻¹ and the reaction step is endothermic with the reaction energy of 14.1 kcal mol⁻¹ (Fig. 4a).

And then, the O₂-enol form structure of 7-methylxanthine, A2-IM_T, is converted into its keto structure, A2-PC, via enol-to-keto tautomerism reaction. One auxiliary water molecule was added to act as a proton bridge, receiving a proton and donating one in turn. As depicted in Fig. 3b, attributed to the presence of the auxiliary water molecule, the transition state A2-TS_T is still a six-membered ring structure. The distances of N₃-C₂, C₂-O₂, O₂-H, H-O_w, O_w-H_{w1}, and H_{w1}-N₃ are 1.347, 1.313, 1.219, 1.226, 1.144 and 1.380 Å, respectively (Fig. 3b). The free energy barrier associated with this step is predicted to be 7.9 kcal mol⁻¹ and the reaction step is exothermic with the reaction energy of 9.2 kcal mol⁻¹ (Fig. 5a), implying that the keto form structure of 7-methylxanthine (A2-PC) is more stable than its O₂-enol form (A2-IM_T) and the enol-to-keto tautomerism reaction is thermodynamically and kinetically favorable.

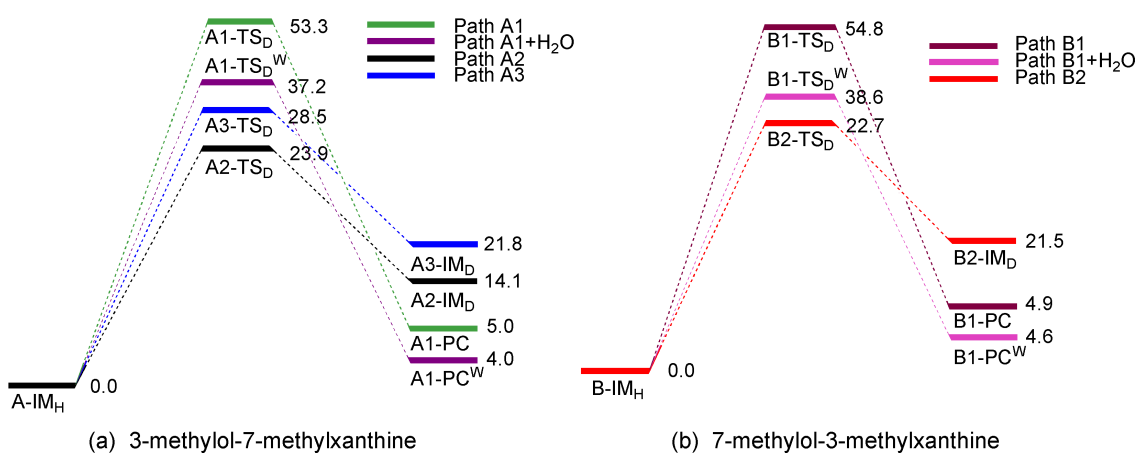


Fig. 4. Energy profiles (free energies in kcal mol⁻¹) for the nonenzymatic fission of C-N bond in 3-methylol-7-methylxanthine (a) and 7-methylol-3-methylxanthine (b) at UB3LYP-D3 functional with B3 basis set.

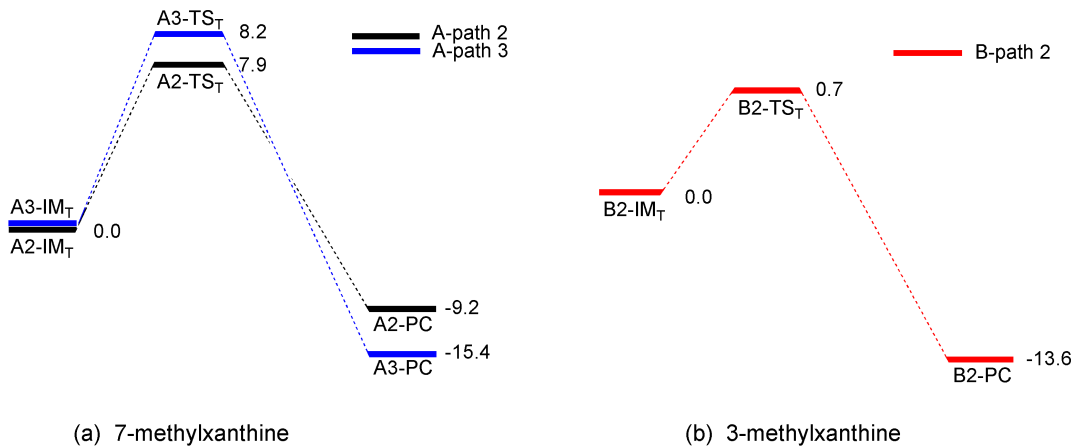


Fig. 5. Energy profiles (free energies in kcal mol^{-1}) for the nonenzymatic enol-to-keto tautomerism reaction in enol form structure of 7-methylxanthine (a) and 3-methylxanthine (b) at UB3LYP-D3 functional with B3 basis set.

Path A3

Analogous to path A2, path A3 is also stepwise, including the initial proton transfer and the following tautomerism processes. Path A3 diverges from path A2 in the yield of 7-methylxanthine isomer (A3-IM_D), formed by the transfer of the proton from hydroxyl oxygen to the contiguous heteroatom N₉ atom via A3-TS_D. The transition state A3-TS_D is a six-membered ring structure formed by N₃, C₃, O, H, N₉ and C₄ atoms (Fig. 3c), whose imaginary vibrational model mainly corresponds to the transfer of proton (H) from O to N₉ atoms accompanied with the breakage of N₃-C₃ bond. The distances of N₃-C₃, C₃-O, O-H, H-N₉, N₉-C₄ and C₄-N₃ are 1.888, 1.301, 1.531, 1.082, 1.389 and 1.341 Å, respectively. The free energy barrier of A3-TS_D is predicted to be 28.5 kcal mol^{-1} and the reaction step is greatly endothermic with the reaction energy of 21.8 kcal mol^{-1} (Fig. 4a).

The next step along path A3 is a tautomerism process, which transforms 7-methylxanthine isomer (A3-IM_T) into its keto form structure (A3-PC). Similarly, one auxiliary water molecule was added to act as a proton bridge to reduce the angle strain. As presented in Fig. 3c, transition state A3-TS_T involved a six-membered ring structure due to the mediation of the auxiliary water molecule. The distances of N₃-C₄, C₄-N₉, N₉-H, H-O_w, O_w-H_{w1}, and H_{w1}-N₃ are 1.350, 1.390, 1.216, 1.292, 1.178 and 1.344 Å, respectively. The free energy barrier required for this step is predicted to be 8.2 kcal mol^{-1} and the reaction step is still greatly exothermic with the reaction energy of 15.4 kcal mol^{-1} (Fig. 5a). Thus, the tautomerism reaction is also thermodynamically and kinetically plausible.

In summary, path A2 is the optimum process for the C-N fission of 3-methylol-7-methylxanthine due to its lowest energy barrier, and then path A3. Therefore, the decomposition of 3-methylol-7-methylxanthine is prone to the contiguous heteroatom-assisted

proton transfer. The direct proton transfer towards N₃ atom pathway (path A1), however, is unfavorable even with the assistance of one auxiliary water molecule. This observation is in accordance with the NBO results. The NPA charges of N₃, O₂ and N₉ atom in A-IM_H are 0.46, 0.61 and 0.54, respectively. The strongest electronegativity of O₂ atom compared with N₃ and N₉ atom makes it easier to accept a proton and results in its lower energy barrier.

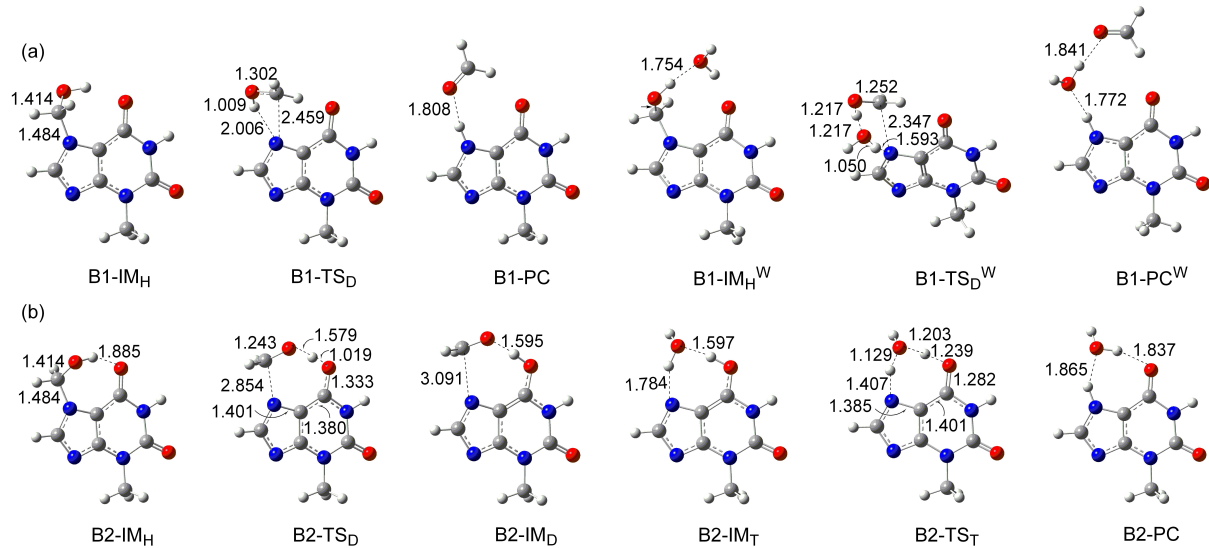


Fig. 6. Optimized structures of the stationary points for the nonenzymatic fission of C-N bond in 3-methylol-7-methylxanthine (bond length in Å).

3.2.2 Fission of C-N bond in 7-methylol-3-methylxanthine

After N₇-methyl hydroxylation, 7-methylol-3-methylxanthine (B-IM_H) formed undergoes C-N bond fission via proton transfer, yielding 3-methylxanthine and formaldehyde. As depicted in Scheme 2b, two possible pathways were investigated, denoted as paths B1 and B2, respectively. Fig. 6 depicts the optimized geometries of all the stationary points for paths B1 and B2. The calculated energy profiles are depicted in Figs. 4 and 5.

Path B1

Path B1 is a concert reaction mechanism, which involves the direct proton transfer from hydroxyl oxygen to N₇ atom, leading to the C-N fission. Analogous to path A1, the direct reaction process occurs via a four-membered ring structure B1-TS_D (Fig. 6a), whose free energy barrier, as expected, is greatly high to be 54.8 kcal mol⁻¹ (Fig. 4b). Then, to relax the angle strain in the transition state, the water-mediated mechanism was taken into account. Owning the mediation of one auxiliary water molecule, the transition state B1-TS_D^W identified is a six-membered ring structure formed by N₇, C₇, O, H, O_w and H_{w1} atoms. The vector of the imaginary vibrational frequency of B1-TS_D^W mainly corresponds to the coupling proton transfers of H atom from O to O_w atoms and H_{w1} atom from O_w to N₇ atoms, leading to the cleavage of the C₇-N₇ bond. The distances of N₇-C₇, C₇-O, O-H, H-O_w, O_w-H_{w1} and H_{w1}-N₇

are 2.347, 1.252, 1.217, 1.217, 1.050 and 1.593 Å, respectively (Fig. 6a). The free energy barrier of B1-TS_D^w is 38.6 kcal mol⁻¹ (Fig. 4b), ca. 16.2 kcal mol⁻¹ lower than B1-TS_D, indicating that the six-membered structure facilitates the proton transfer and energy saving owing to its smaller deformation than the four-membered structure. Nevertheless, large energy barrier is still required for the water-mediated mechanism.

Path B2

In contrast to path B1, path B2 is a stepwise reaction mechanism, which includes the proton transfer from hydroxyl oxygen to the contiguous heteroatom O₆ atom to generate the O₆-enol form structure of 3-methylxanthine (B2-IM_D) followed by tautomerism to yield B2-PC. The located transition state B2-TS_D involved in first proton transfer process is a seven-membered ring structure formed by N₇, C₇, O, H, O₆, C₆, and C₅ atoms (Fig. 6b), which mainly corresponds to the transfer of proton (H) from O to O₆ atoms, leading to the breakage of N₇-C₇ bond. The distances of N₇-C₇, C₇-O, O-H, H-O₆, O₆-C₆, C₆-C₅ and C₅-N₇ are 2.854, 1.243, 1.579, 1.019, 1.333, 1.380 and 1.401 Å, respectively. The free energy barrier of B2-TS_D is predicted to be 22.7 kcal mol⁻¹ and the reaction step is endothermic with the reaction energy of 21.5 kcal mol⁻¹ (Fig. 4b).

In the next tautomerism step along path B2, the transition state B2-TS_T characterized is a seven-membered ring structure in the presence of one auxiliary water molecule. The distances of N₇-C₅, C₅-C₆, C₆-O₆, O₆-H, H-O_w, O_w-H_{w1}, and H_{w1}-N₇ are 1.385, 1.401, 1.282, 1.239, 1.203, 1.129 and 1.407 Å, respectively. The free energy barrier associated with this step is predicted to be 0.7 kcal mol⁻¹ and the reaction step is exothermic with the reaction energy of 13.6 kcal mol⁻¹ (Fig. 5b). It indicates that the tautomerism reaction is also thermodynamically and kinetically favorable.

An analysis of the electronic structure of B-IM_H shows that the NPA charges of the O₆ and N₇ atom are -0.64 and -0.38, respectively. It can be seen that the contiguous heteroatom-assisted proton transfer mechanism (path B2) is more favorable than the direct proton transfer mechanism (path B1) and is predicted to be the optimum pathway for the C-N bond fission of 7-methylol-3-methylxanthine.

Taking all the above into account, the N-demethylation mechanism of theobromine proceeds in a HAT process. The rate-determining steps of 3-N and 7-N demethylations both involve the N-methyl hydroxylation. The *N*-demethylation of theobromine favors SSM mechanism and proceeds mainly on the HS quartet state due to its lower free energy with respect to the LS doublet state. 3-N demethylation mechanism on the HS state is the most feasible demethylation mechanism of theobromine and 7-methylxanthine therefore is the optimum demethylation product, which agree well with the experimental results [38]. The N-demethylation is predicted to be under kinetic control [39].

4. Conclusions

Theobromine, a purine alkaloid, is present in many widely consumed drinks and some foods, yet little is known about its metabolism mechanism. In this work, a theoretical analysis of N-demethylation mechanism of theobromine by CYP1A2 has been carried out using density functional theory. Two possible N-demethylation pathways of theobromine were taken into account, i.e. 3-N and 7-N demethylations. The N-demethylation mechanism involves two reaction steps: the initial N-methyl hydroxylation to generate carbinolamine complex and the subsequent carbinolamine decomposition to yield methylxanthine and formaldehyde. Our calculations illustrate that N-methyl hydroxylation is the rate-limiting step on the potential energy surface, which is a hydrogen atom transfer (HAT) step and proceeds in a spin-selective mechanism (SSM), mainly on the HS quartet state. 3-N demethylation is more favorable than 7-N demethylation attributed to its lower free energy. Consequently, 7-methylxanthine is the optimum demethylation product of theobromine, which agrees with the experimental observation. Furthermore, the decompositions of carbinolamines in 3-N and 7-N demethylations are both prone to the contiguous heteroatom-assisted proton-transfer process. The most favorable decomposition pathway involves the proton transfer from hydroxyl oxygen to the adjacent heteroatom O₂ atom for 3-N demethylation and O₆ atom for 7-N demethylation. This work has investigated the mechanism of N-demethylation of theobromine and explored the optimal product and the major reaction path at the theoretical level, which can provide more significant information about the metabolism of purine alkaloid and important clues for the experimental study.

Supporting Information

Cartesian coordinates of all stationary points along the potential energy profiles.

Acknowledgments

This work was supported by grants from National Natural Science Foundation of China (Grant No. 21203153), Science & Technology Department (Grant No. 2011JY0136) and Department of Education (Grant No. 12ZA174) of Sichuan Province and China West Normal University (Grant No. 11B002).

References

- [1] H.I.C. Lowe, C.T. Watson, S. Badal, P. Peart, N.J. Toyang, J. Bryant, Promising efficacy of the *cola acuminata* plant: a mini review, *Adv. Biol. Chem.* 4 (2014) 240-245.
- [2] L.C. Carrillo, J. Londoño-Londoño, A. Gil, Comparison of polyphenol, methylxanthines and antioxidant activity in *theobroma cacao* beans from different cocoa-growing areas in colombia, *Food Res. Int.* 60 (2014) 273-280.

- [3] J. Li, Y.-L. Wei, Y.-Y. Li, L. Pang, W.-W. Deng, C.-J. Jiang, A correlation study of caffeine content with theobromine content, cSNPs, and transcriptional expression of three genes in tea plants, *Crop. Sci.* 54 (2014) 1124-1132.
- [4] L. Geraets, H.J. Moonen, E.F. Wouters, A. Bast, G.J. Hageman, Caffeine metabolites are inhibitors of the nuclear enzyme poly(ADP-ribose)polymerase-1 at physiological concentrations, *Biochem. Pharmacol.* 72 (2006) 902-910.
- [5] M. Windholz, The merck index of chemicals and drugs, 9th ed., Merck & Co., Rahway, NJ, 1976, pp. 1625, 8896 and 8897.
- [6] H.J. Smit, E.A. Gaffan, P.J. Rogers, Methylxanthines are the psycho-pharmacologically active constituents of chocolate, *Psychopharmacology (Berl)* 176 (2004) 412-419.
- [7] O.S. Usmani, M.G. Belvisi, H.J. Patel, N. Crispino, M.A. Birrell, M. Korbonits, D. Korbonits, P.J. Barnes, Theobromine inhibits sensory nerve activation and cough, *FASEB J.* 19 (2005) 231-233.
- [8] S. Scheindlin, A new look at the xanthine alkaloids, *Mol. Interventions* 7 (2007) 236-242.
- [9] B. Stavric, Methylxanthines:toxicity to humans.3.theobromine,paraxanthine and the combined effects of methylxanthines, *Food Chem. Toxic.* 26 (1988) 725-733.
- [10] J.B. Thomas, J.H. Yen, M.M. Schantz, B.J. Porter, K.E. Sharpless, Determination of caffeine, theobromine, and theophylline in standard reference material 2384, baking chocolate, using reversed-phase liquid chromatography, *J. Agric. Food. Chem.* 52 (2004) 3259-3263.
- [11] R. Devi, J. Narang, S. Yadav, C.S. Pundir, Amperometric determination of xanthine in tea, coffee, and fish meat with graphite rod bound xanthine oxidase, *J. Anal. Chem.* 67 (2012) 273-277.
- [12] R. Franco, A. Oñatibia-Astibia, E. Martínez-Pinilla, Health benefits of methylxanthines in cacao and chocolate, *Nutrients* 5 (2013) 4159-4173.
- [13] J.A. Clancy, S.A. Deuchars, J. Deuchars, The wonders of the wanderer, *Exp. Physiol.* 98 (2013) 38-45.
- [14] P. Rydberg, U. Ryde, L. Olsen, Sulfoxide, sulfur, and nitrogen oxidation and dealkylation by cytochrome P450, *J. Chem.Theory. Comput.* 4 (2008) 1369-1377.
- [15] K.A. Miller, M.G. Assuncao, N.J. Dangerfield, S.M. Bandiera, P.S. Ross, Assessment of cytochrome P450 1A in harbour seals (*Phoca vitulina*) using a minimally-invasive biopsy approach, *Mar. Environ. Res.* 60 (2005) 153-169.
- [16] O. Pelkonen, M. Turpeinen, J. Hakkola, P. Honkakoski, J. Hukkanen, H. Raunio, Inhibition and induction of human cytochrome P450 enzymes: current status, *Arch. Toxicol.* 82 (2008) 667-715.
- [17] J. Wojcikowski, P. Maurel, W.A. Daniel, Characterization of human cytochrome p450 enzymes involved in the metabolism of the piperidine-type phenothiazine neuroleptic thioridazine, *Drug Metab. Dispos.* 34 (2006) 471-476.
- [18] J. Wojcikowski, L. Pichard-Garcia, P. Maurel, W.A. Daniel, Contribution of human cytochrome p-450 isoforms to the metabolism of the simplest phenothiazine neuroleptic promazine, *Br. J. Pharmacol.* 138 (2003) 1465-1474.

- [19] I. Ayari, U. Fedeli, S. Saguem, S. Hidar, S. Khlifi, S. Pavanello, Role of CYP1A2 polymorphisms in breast cancer risk in women, *Mol. Med. Rep.* 7 (2013) 280-286.
- [20] S.S.M. Yip, R.A. Coulombe Jr., Molecular cloning and expression of a novel cytochrome P450 from turkey liver with aflatoxin B1 oxidizing activity, *Chem. Res. Toxicol.* 19 (2006) 30-37.
- [21] M.J. Arnaud, Pharmacokinetics and metabolism of natural methylxanthines in animal and man, *Handb. Exp. Pharmacol.* 200 (2011) 33-91.
- [22] S.S. Dash, S.N. Gummadi, Catabolic pathways and biotechnological applications of microbial caffeine degradation, *Biotechnol. Lett.* 28 (2006) 1993-2002.
- [23] J. Dorne, K. Walton, A.G. Renwick, Uncertainty factors for chemical risk assessment: human variability in the pharmacokinetics of CYP1A2 probe substrates, *Food Chem. Toxicol.* 39 (2001) 681-696.
- [24] N. Rodopoulos, L. Höjvall, A. Norman, Elimination of theobromine metabolites in healthy adults, *Scand. J. Clin. Invest.* 56 (1996) 373-383.
- [25] A.H. Meyer, A. Dybala-Defratyka, P.J. Alaimo, I. Geronimo, A.D. Sanchez, C.J. Cramer, M. Elsner, Cytochrome P450-catalyzed dealkylation of atrazine by *Rhodococcus* sp. strain NI86/21 involves hydrogen atom transfer rather than single electron transfer, *Dalton Trans.* 43 (2014) 12175-12186.
- [26] M.A. Cerny, R.P. Hanzlik, Cytochrome P450-catalyzed oxidation of N-benzyl-N-cyclopropylamine generates both cyclopropanone hydrate and 3-hydroxypropionaldehyde via hydrogen abstraction, not single electron transfer, *J. Am. Chem. Soc.* 128 (2006) 3346-3354.
- [27] F.P. Guengerich, C.H. Yun, T.L. Macdonald, Evidence for a 1-electron oxidation mechanism in N-dealkylation of N,N-dialkylanilines by cytochrome P450 2B1, *J. Biol. Chem.* 27 (1996) 27321-27329.
- [28] S. Shaik, S.P.d. Visser, F. Ogliaro, H. Schwarz, D. Schröder, Two-state reactivity mechanisms of hydroxylation and epoxidation by cytochrome P-450 revealed by theory, *Curr. Opin. Chem. Biol.* 6 (2002) 556-567.
- [29] Z. Fu, Y. Wang, Z. Wang, H. Xie, J. Chen, Transformation pathways of isomeric perfluorooctanesulfonate precursors catalyzed by the active species of P450 enzymes: in silico investigation, *Chem. Res. Toxicol.* (2014).
- [30] D. Li, Y. Wang, K. Han, C.G. Zhan, Fundamental reaction pathways for cytochrome P450-catalyzed 5'-hydroxylation and N-demethylation of nicotine, *J. Phys. Chem. B.* 114 (2010) 9023-9030.
- [31] D. Li, Y. Wang, C. Yang, K. Han, Theoretical study of N-dealkylation of N-cyclopropyl-N-methylaniline catalyzed by cytochrome P450: insight into the origin of the regioselectivity, *Dalton Trans.* 2 (2009) 291-297.
- [32] Y. Wang, D. Kumar, C. Yang, K. Han, S. Shaik, Theoretical study of N-demethylation of substituted N,N-dimethylanilines by cytochrome P450: the mechanistic significance of kinetic isotope effect profiles, *J. Phys. Chem. B* 111 (2007) 7700-7710.
- [33] S. Sansen, J.K. Yano, R.L. Reynald, G.A. Schoch, K.J. Griffin, C.D. Stout, E.F. Johnson, Crystal structure of human microsomal P450 1A2 in complex with alpha-naphthoflavone, *J. Biol. Chem.* 282 (2007) 14348-14355.
- [34] R. DenningtonII, T. Keith, J. Millam, K. Eppinnett, W.L. Hovell, R. Gilliland, Gauss View, Version 3.0,

Semicem Inc, Shawnee Mission, 2003.

[35] M.J. Frisch, G.W. Trucks, H.B. Schlegel, G.E. Scuseria, M.A. Robb, J.R. Cheeseman, G. Scalmani, V. Barone, B. Mennucci, G.A. Petersson, H. Nakatsuji, M. Caricato, X. Li, H.P. Hratchian, A.F. Izmaylov, J. Bloino, G. Zheng, J.L. Sonnenberg, M. Hada, M. Ehara, K. Toyota, R. Fukuda, J. Hasegawa, M. Ishida, T. Nakajima, Y. Honda, O. Kitao, H. Nakai, T. Vreven, J.J.A. Montgomery, J.E. Peralta, F. Ogliaro, M. Bearpark, J.J. Heyd, E. Brothers, K.N. Kudin, V.N. Staroverov, R. Kobayashi, J. Normand, K. Raghavachari, A. Rendell, J.C. Burant, S.S. Iyengar, J. Tomasi, M. Cossi, N. Rega, N.J. Millam, M. Klene, J.E. Knox, J.B. Cross, V. Bakken, C. Adamo, J. Jaramillo, R. Gomperts, R.E. Stratmann, O. Yazyev, A.J. Austin, R. Cammi, C. Pomelli, J.W. Ochterski, R.L. Martin, K. Morokuma, V.G. Zakrzewski, G.A. Voth, P. Salvador, J.J. Dannenberg, S. Dapprich, A.D. Daniels, O. Farkas, J.B. Foresman, J.V. Ortiz, J. Cioslowski, D.J. Fox, Gaussian 09, Revision D01, Gaussian Inc, Wallingford, 2013.

[36] H.P. Hratchian, H.B. Schlegel, Accurate reaction paths using a hessian based predictor-corrector integrator, *J. Chem. Phys.* 120 (2004) 9918-9924.

[37] K. Fukui, The path of chemical reactions-the IRC approach, *Acc. Chem. Res.* 14 (1981) 363-368.

[38] N. Khan, N.M. Nicod, Biomarkers of cocoa consumption. in chocolate and health, Springer Milan 2012 (2012) 33-40.

[39] M. Hada, Y. Tanaka, M. Ito, M. Murakami, H. Amii, Y. Ito, H. Nakatsuji, Theoretical study on the reaction mechanism and regioselectivity of silastannation of acetylenes with a palladium catalyst, *J. Am. Chem. Soc.* 116 (1994) 8754-8765.

Table 1 Free energy barriers (in kcal mol⁻¹) in the gas phase calculated for the N-methyl hydroxylation of theobromine using different functionals with the B2 and B3 basis sets.

	N ₃ -methyl hydroxylation			N ₇ -methyl hydroxylation			Free energy barrier difference ^a
	HS	LS	LS-HS ^b	HS	LS	LS-HS ^b	
B2 basis set							
UB3LYP	18.5	21.1	2.6	22.1	23.0	0.9	3.6
UB3LYP-D3	16.0	18.4	2.4	17.9	21.6	3.7	1.9

B3 basis set

UB3LYP	15.7	18.0	2.3	19.2	20.1	0.9	3.5
UB3LYP-D3	13.2	15.2	2.0	15.0	18.7	3.7	1.8
UB3PW91-D3	10.6	13.5	2.9	14.6	17.1	2.5	4.0
UPBE1PBE-D3	10.0	12.6	2.6	14.1	18.8	4.7	4.1

^a The difference between the lowest barriers calculated for the two reaction pathways.

^b The difference between the LS and HS.

Table 2 Spin densities for the species in the N–methyl hydroxylation of theobromine by Cpd I of CYP1A2.

	Cytochrome				Theobromine			
	Fe	O	SH	Por	H	C	N	Rest
A- ² RC	1.20	0.90	-0.58	-0.52	0.00	0.00	0.00	0.00
A- ⁴ RC	1.07	0.95	0.53	0.45	0.00	0.00	0.00	0.00
A- ² TS _H	0.98	0.33	-0.22	-0.57	-0.04	0.46	0.00	0.06
A- ⁴ TS _H	1.25	0.64	0.39	0.16	-0.05	0.51	0.03	0.07
A- ⁴ IM	1.85	0.25	0.02	-0.12	0.00	0.93	-0.03	0.10
A- ² IM _H	1.11	0.00	-0.02	-0.09	0.00	0.00	0.00	0.00
A- ⁴ IM _H	2.92	0.01	0.10	-0.03	0.00	0.00	0.00	0.00
B- ² RC	1.26	0.84	-0.58	-0.52	0.00	0.00	0.00	0.00
B- ⁴ RC	1.12	0.90	0.52	0.45	0.00	0.00	0.00	0.00
B- ² TS _H	1.00	0.50	-0.46	-0.54	-0.06	0.49	-0.02	0.09
B- ⁴ TS _H	1.69	0.54	0.06	0.10	-0.04	0.54	-0.01	0.11
B- ⁴ IM	1.88	0.23	0.01	-0.12	0.00	0.90	-0.11	0.20
B- ² IM _H	1.10	0.00	-0.02	-0.09	0.00	0.00	0.00	0.00
B- ⁴ IM _H	2.95	0.01	0.06	-0.02	0.00	0.00	0.00	0.00

^a Por = porphyrine.